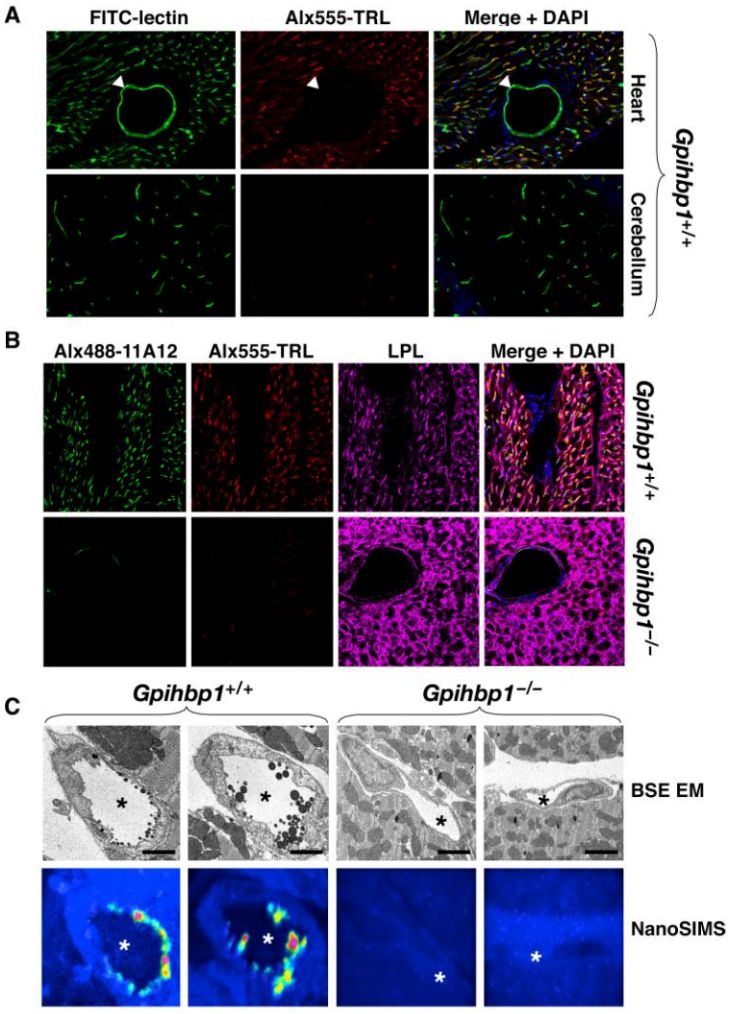


**Figure S1. Triglyceride-rich lipoprotein (TRL) binding parallels GPIHBP1 expression. Related to Figure 1.** (A) Fluorescence microscopy images showing TRL binding (red) in small blood vessels (green) but absent in large blood vessels (arrowhead), and in the cerebellum, a tissue that does not express GPIHBP1 (Davies et al., 2010). (B) Fluorescence microscopy images showing that TRL binding (red) closely matched the staining patterns for GPIHBP1 (green) and LPL (magenta) in the heart of a wild-type mouse. (C) NanoSIMS analysis showing TRL binding to capillary endothelial cells in a wild-type mouse but not in a *Gpihbp1*$^{-/-}$ mouse. Capillary lumens are identified with an asterisk.

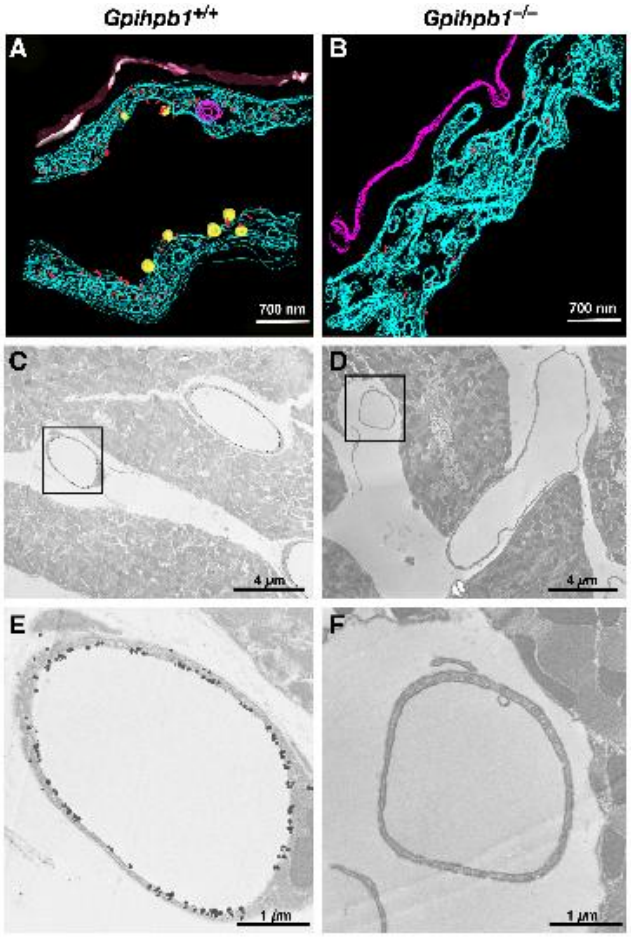


**Figure S2. Distribution of nanovilli, TRL binding, and GPIHBP1 expression in heart capillaries. Related to Figure 3.** (A, B) 3-D modeling of 131 individual EM tomograms revealed multiple TRLs attached to the endothelial cell surface in *Gpihbp1*$^{+/+}$ but not *Gpihbp1*$^{-/-}$ mice. Contour lines were drawn to outline TRLs (yellow), myocytes (magenta), endothelial cell membranes (blue), and nanovilli (red), on endothelial cells. (C, D) Low-magnification and (E, F) high-magnification transmission EM images showing many gold particles (GPIHBP1) in capillaries of the wild-type mouse (C, E) but none in the *Gpihbp1*$^{-/-}$ mouse (D, F). The boxed areas in panels C and D are shown at higher magnification in panels E and F, respectively.

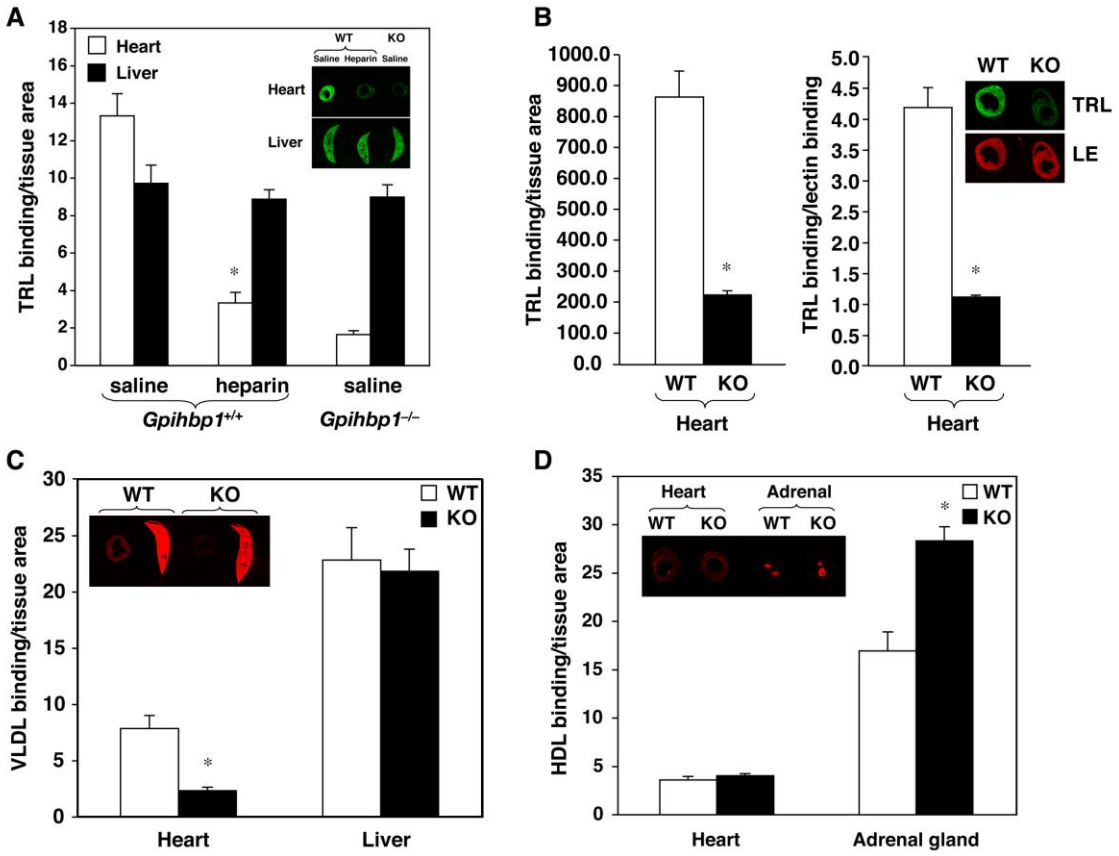


**Figure S3. The margination of TRLs in the heart is heparin-sensitive, dependent on GPIHBP1 expression, and specific. Related to Figure 4.** (A) Heparin (100 U) reduced the amount of TRL binding in wild-type mice to levels observed in saline-injected *Gpihbp1*$^{-/-}$ mice. ∗, $p < 0.01$ (*vs* saline). (B) TRL binding was lower in *Gpihbp1*$^{-/-}$ hearts than in wild-type mouse hearts after normalization to tissue area (left) or endothelial cell content as judged by lectin (LE) binding (right). ∗, $p < 0.01$ (wild-type *vs* knockout). (C) The binding of both TRLs (not shown) and human VLDL in the heart was lower in *Gpihbp1* knockout mice (reduced by 71% for VLDL and 72% for TRLs). ∗, $p < 0.01$ (wild-type *vs* knockout). (D) HDL binding was very low in the heart but high in the adrenal gland. The absence of GPIHBP1 did not reduce HDL binding in either tissue. ∗, $p < 0.01$ (wild-type *vs* knockout).

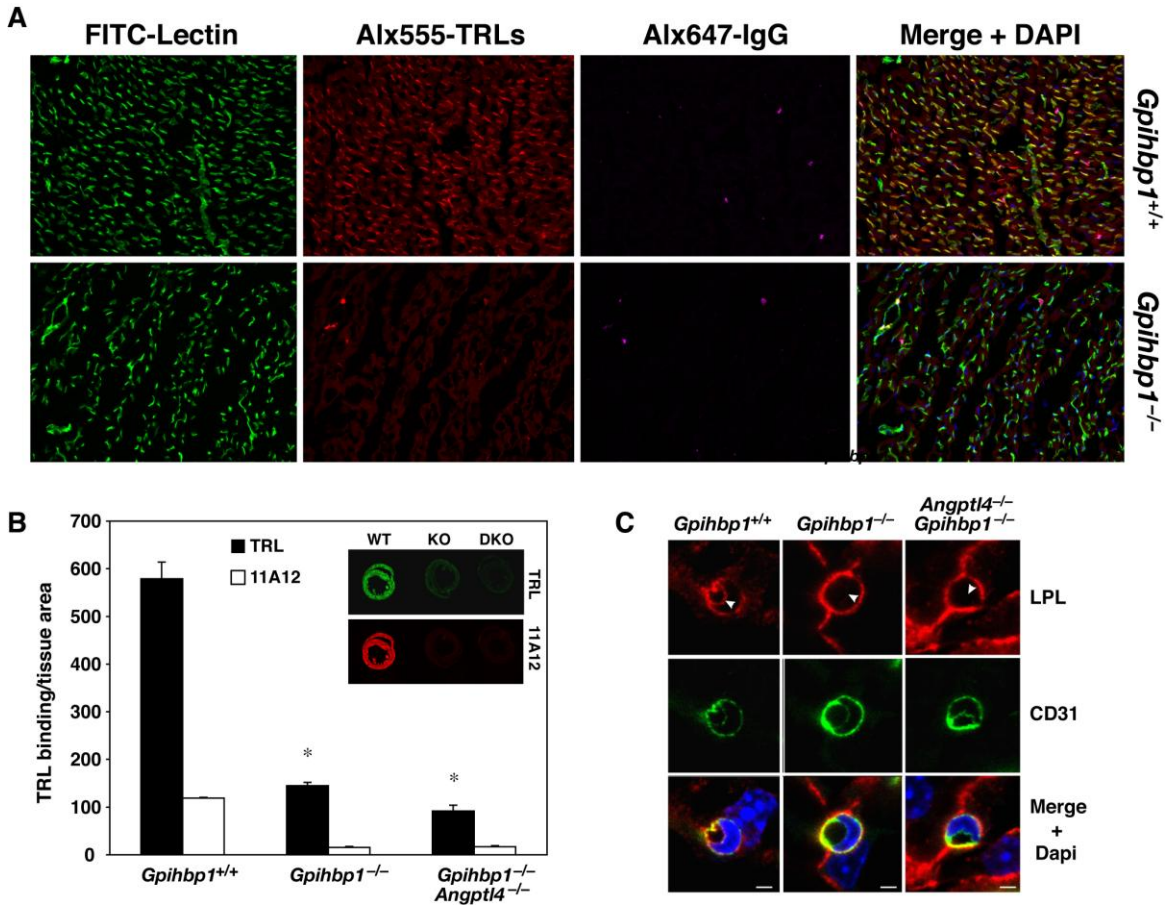


**Figure S4. The reduced binding of TRLs in *Gpihbp1*$^{-/-}$ mouse hearts is not due to high plasma triglyceride levels. Related to Figure 4.** (A) Isolated hearts from *Gpihbp1*$^{+/+}$ and *Gpihbp1*$^{-/-}$ mice were cannulated and perfused with FITC-labeled lectin (green), Alexa555-labeled TRLs (red), and Alexa647-labeled rat IgG. TRL binding was detected in wild-type hearts and colocalized with endothelial cells. The binding was eliminated when heparin was included in the perfusion solution (not shown). In *Gpihbp1*$^{-/-}$ mice, TRL binding was low. There were areas that were "positive" for TRLs, but those coincided with areas of incomplete perfusion, as judged by Alexa647-IgG staining (magenta). (B) ANGPTL4 deficiency does not increase TRL binding in *Gpihbp1*$^{-/-}$ mice. *Angptl4*-deficiency has been reported to reduce plasma triglyceride levels in *Gpihbp1*$^{-/-}$ mice (Sonnenburg et al., 2009). In our studies, fasting plasma triglyceride levels

were 1742 mg/dl in *Gpihbp1*$^{-/-}$ mice *vs*. 132 mg/dl in *Gpihbp1*$^{-/-}$*Angptl4*$^{-/-}$ mice. However, the margination of IR-dye–labeled TRLs was not greater in heart capillaries of *Gpihbp1*$^{-/-}$*Angptl4*$^{-/-}$ mice. ∗, $p < 0.01$ (*vs Gpihbp1*$^{+/+}$). (C) Confocal fluorescence microscopy images of cross sections through an endothelial cell nucleus, stained with DAPI (blue), were captured on a confocal microscope with a 63× objective and 3× optical zoom. LPL (green) was absent from the luminal face of endothelial cells in both *Gpihbp1*$^{-/-}$ and *Gpihbp1*$^{-/-}$*Angptl4*$^{-/-}$ mice. The locations of the capillary lumens are identified with arrowheads.

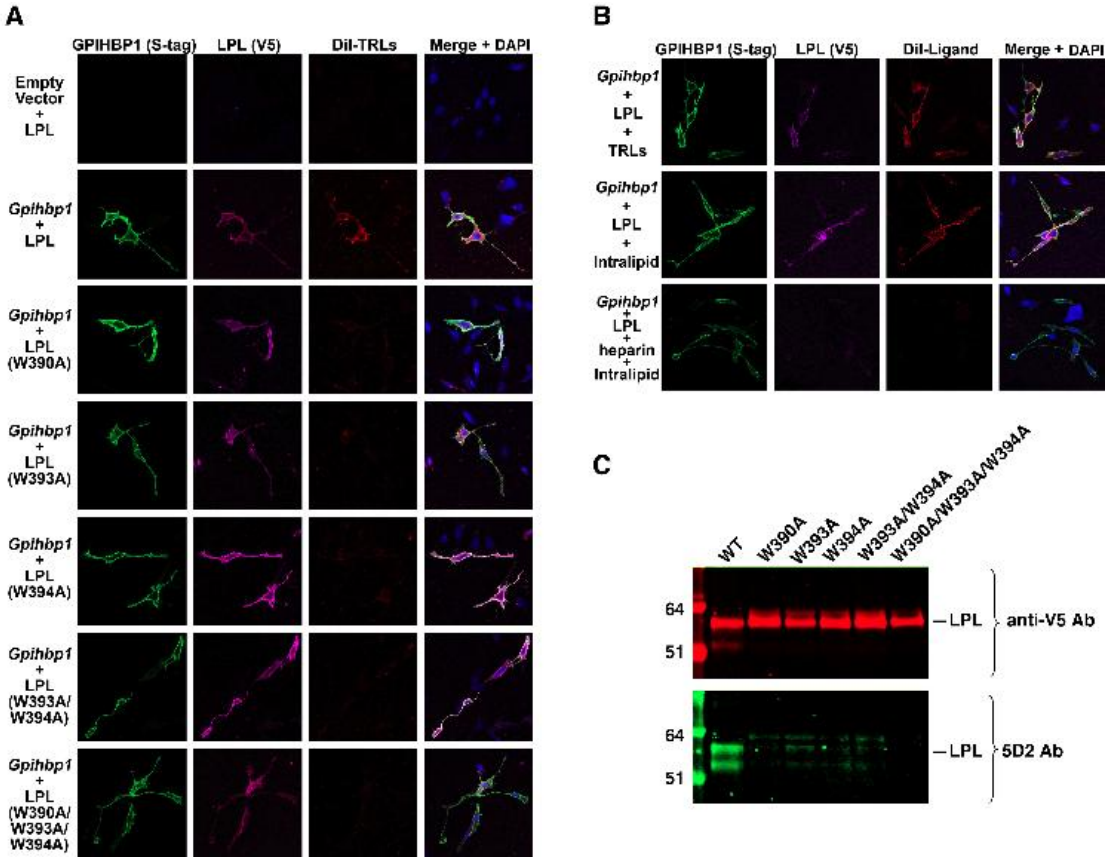


**Figure S5. Immunofluoresence microscopy showing that the binding of TRLs to GPIHBP1-bound LPL depends on a cluster of tryptophans in LPL's carboxyl-terminal domain and that the binding of Intralipid to GPIHBP1-bound LPL is sensitive to heparin. Related to Figure 5.** (A) CHL-11 cells were transfected with GPIHBP1 (green) and the binding of DiI-labeled TRLs (red) measured after the addition of wild-type LPL or different LPL mutants (as indicated) (magenta). TRLs only bound to cells that had wild-type LPL on their cell surface. (B) The binding of DiI-labeled Intralipid particles (red) to GPIHBP1-expressing cells (green) incubated with wild-type LPL (magenta) was blocked by heparin. (C) Western blot analysis showing that mutagenesis of the tryptophan cluster in the carboxyl terminus of LPL inhibits antibody 5D2 binding.

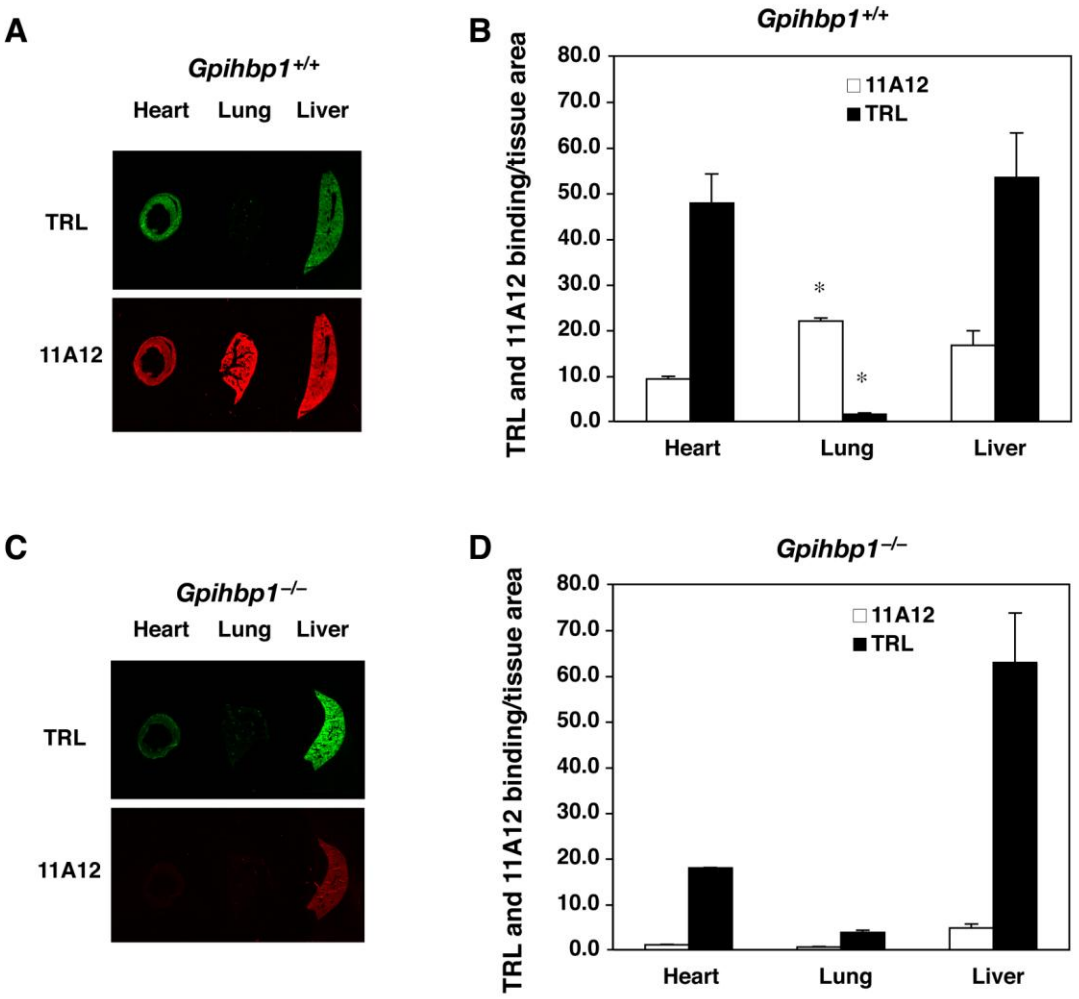


**Figure S6. TRLs bind poorly in the lung despite high levels of GPIHBP1 expression. Related to Figure 6.** (A, B) Images of representative tissue sections, and quantitative data showing high GPIHBP1 expression (as detected by antibody 11A12, red) but very low levels of TRL binding (green) in the lungs of wild-type mice. ∗, $p < 0.01$ (*vs* heart). (C, D) Images of representative tissue sections, and quantitative data showing very little antibody 11A12 binding or TRL binding in the lungs of *Gpihbp1*$^{-/-}$ mice.

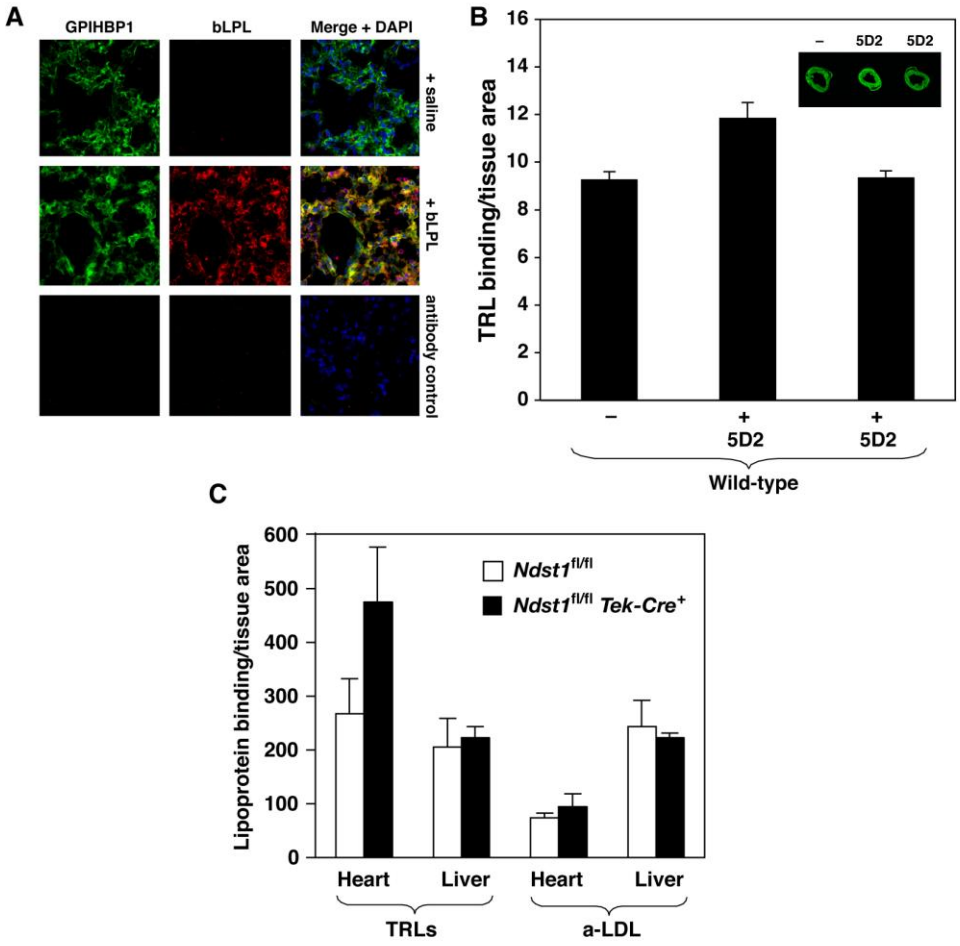


**Figure S7. Bovine LPL, when injected intravenously, is captured by capillaries of the lung of wild-type mice. Inhibition of HSPG sulfation does not inhibit TRL margination in the heart. Related to Figures 6 & 7.** (A) Immunofluorescence microscopy images showing the capture of injected bovine LPL (red) by endothelial cells in the lung. (B) Quantitative measurements showing that antibody 5D2 does not reduce TRL binding in wild-type mice. Representative image of heart tissue sections is shown in the inset. (C) Quantitative analyses showing that *Ndst1*-deficiency does not reduce TRL or a-LDL binding in the heart (or liver).